

## Modelling radiation-induced cell cycle delays

Anna Ochab-Marcinek · Ewa  
Gudowska-Nowak · Elena Nasonova · Sylvia  
Ritter

Received: date / Accepted: date

**Abstract** Ionizing radiation is known to delay the cell cycle progression. In particular after particle exposure significant delays have been observed and it has been shown that the extent of delay affects the expression of damage such as chromosome aberrations. Thus, to predict how cells respond to ionizing radiation and to derive reliable estimates of radiation risks, information about radiation-induced cell cycle perturbations is required. In the present study we describe and apply a method for retrieval of information about the time-course of all cell cycle phases from experimental data on the mitotic index only. We study the progression of mammalian cells through the cell cycle after exposure. The analysis reveals a prolonged block of damaged cells in the G2 phase. Furthermore, by performing an error analysis on simulated data valuable information for the design of experimental studies has been obtained. The analysis

---

This work was supported in part (A. O-M) by the grant of Polish State Committee for Scientific Research (KBN, Grant No 1 P03B 159 29). Moreover, E. G-N acknowledges Marie Curie TOK COCOS grant at the Mark Kac Complex Systems Research Center in Kraków, Poland. E.N. was supported by BMBF (Bonn, Germany) under contract number 02S8203 and 02S8497.

---

A. Ochab-Marcinek  
Department of Soft Condensed Matter, Institute of Physical Chemistry, Polish Academy of Sciences, ul. Kasprzaka 44/52, Warsaw, Poland  
E-mail: ochab@ifka.ichf.edu.pl

E. Gudowska-Nowak  
Marian Smoluchowski Institute of Physics, Jagiellonian University, ul. Reymonta 4, Kraków, Poland  
Mark Kac Complex Systems Research Centre, Jagiellonian University, Reymonta 4, Kraków, Poland  
Biophysics Department, Gesellschaft für Schwerionenforschung (GSI), Planckstrasse 1, Darmstadt, Germany

E. Nasonova  
Biophysics Department, Gesellschaft für Schwerionenforschung (GSI), Planckstrasse 1, Darmstadt, Germany  
Joint Institute for Nuclear Research (JINR), 141980 Dubna, Moscow Region, Russia

S. Ritter  
Biophysics Department, Gesellschaft für Schwerionenforschung (GSI), Planckstrasse 1, Darmstadt, Germany

---

showed that the number of cells analyzed in an experimental sample should be at least 100 to obtain a relative error less than 20%.

**Keywords** ionizing radiation · cell cycle delay · Monte Carlo simulation

## 1 Introduction

It is well-known that cells respond to DNA damage by activating checkpoints that delay the cell cycle transition in particular from G1 to S phase and from G2 to M phase. These delays are assumed to allow additional time for repair (Li and Zou (2005)).

After sparsely ionizing radiation such as X-rays or  $\gamma$ -rays mild perturbations of the cell kinetics have been observed corresponding to the delay of about 1 hour per 1 Gy of exposure (Purrot et al (1980)). In contrast, after particle irradiation dramatic cell cycle delays have been measured lasting up to 3 cell generation times (Scholz et al (1994) and references therein). Moreover, a rapid desynchronization of initially synchronous cell populations has been observed after particle exposure (Scholz et al (1994); Ritter et al (1996, 2000)). The differences between the effects induced by both radiation qualities may be directly attributed to spatial differences in the energy deposition (Ritter et al (2000); Gudowska-Nowak et al (2005)).

Cell cycle delays as observed after radiation exposure are important for the interpretation of other biological experiments. For example, recent reports have shown that cell cycle delays interfere with the time-course of aberrations visible in cells at the first mitosis post-irradiation. In particular, after particle exposure which delays the cell cycle progression more than sparsely ionizing radiation, a drastic increase in the aberration yield with sampling time has been observed (Ritter et al (1996, 2000)) and it has been recently shown that the average time to enter the first mitosis correlates directly with the aberration burden of a cell (Gudowska-Nowak et al (2005)). In other words, cells entering mitosis at later times harbor more aberrations than those entering mitosis earlier. Since the frequency of aberrations expressed in first cycle metaphases is used to determine the absorbed dose (e.g. Cucinotta and Durante (2006)) and to derive cancer risk estimates (e.g. Mateuca et al (2006)), the damage sustained by the whole cell population has to be determined. This can be achieved by the analysis of samples collected at multiple sampling times covering the whole interval from the first to the last cells reaching mitosis. Then, the total yield of aberrations can be determined by a mathematical approach (i.e. integration analysis, see Kaufman et al (1974); Scholz et al (1998)).

Experimental and theoretical studies of the cell cycle progression are also of primary interest in the context of cancer therapy (Hahnfeldt and Hlatky (1996); Montalenti et al (1998); Erba et al (2002); Basse and Ubezio (2007); Wilson (2007)), since the therapeutic response of solid tumors is known to depend not only on the administered dose of ionizing radiation or chemotherapy agents but also on repopulation and redistribution of cancerous cells. Cancer therapies may target specific phases of the cell cycle by blocking or delaying the progress through one or more phases (see Montalenti et al (1998)).

The specific aim of our project was to further elucidate the complexity of particle-induced cell cycle arrest. Investigations into the effects of particles are becoming increasingly pertinent in light of rapidly growing interest in this type of radiotherapy

---

(Amaldi and Kraft (2007)). Furthermore, for the planning of manned missions to Moon and Mars, a better knowledge of the action of charged particles is needed, since the main contribution of dose during a space mission outside the magnetic shielding of the Earth originates from galactic cosmic rays, which are heavy particles from the most frequent protons to up to iron ions (Cucinotta and Durante (2006)).

In this study, we present a method for retrieval of information about all previous phases of the cell cycle, when only the mitotic index of the experimental cell sample is known. We use the method to analyze the data measured for mammalian V79 cells after exposure to Ar ions (Ritter et al (2000)). V79 cells represent a frequently used model system to study genotoxic effects of ionizing radiation (Ritter et al (1996, 2000); Weyrather et al (1999); Groesser et al (2007); Pathak et al (2007)) or chemical agents (Virgilio et al (2004)). Information on the cell cycle progression was available in the form of subsequent measurements of the mitotic index in control and irradiated samples (Fig. 2) and duration times of cell cycle phases of control cells (Sinclair (1969); Scholz (2003)). Since in the experiment not only the mitotic index, but also the aberration yield has been measured, the approach may allow us to study in future the progression of cells carrying a different number of aberrations.

Mitotic index is the measure of the number of cells undergoing mitosis at a given time. As the duration of cell cycle phases varies from cell to cell, the mitotic index depends on the duration distribution of mitosis, but also on the corresponding duration distributions of the previous phases. We retrieve these distributions using a multi-dimensional fit based on general assumptions concerning the distribution shape, which are inferred from other experiments (Montalenti et al, 1998). In this way, having only the mitotic indices for control and irradiated cells, we were able to compare their progression through the whole cell cycle and predict which phases are most vulnerable to irradiation. The fitted parameters of the duration distributions of cell cycle phases have also been used to estimate the experimental error of the mitotic index measurement, depending on the number of cells in the sample. The estimation has been carried out using the Monte Carlo simulation of the cell cycle progression for a given number of cells.

## 2 Materials and methods

### 2.1 Experimental data used for the analysis

To examine in more detail charged particle-induced cell cycle progression delays in the first post-irradiation cycle, previously published data were reanalysed (Ritter et al (2000)).

For the experiment, V79 Chinese hamster cells were synchronized by mitotic shake off, a method based on the selective detachment of mitotic cells from monolayers by shaking. Mitotic cells were plated in Petri dishes and about 2h after seeding, when the cells had attached and divided and progressed into G1-phase, the exposure was done.

Irradiation with  $10.4 \text{ MeV u}^{-1}$  Ar ions ( $\text{LET} = 1226 \text{ keV}\mu\text{m}^{-1}$ ) was performed with a fluence of  $10^6$  particles  $\text{cm}^{-2}$  corresponding to a dose of 1.96 Gy, respectively. At the time of irradiation, at least 95% of cells were in G1 phase as determined by flow cytometry. Immediately after exposure, 5'-Bromo-2'-deoxyuridine ( $10 \mu\text{mg ml}^{-1}$ ) was added to the samples to distinguish between metaphases in the different post-irradiation cycles. Cells were harvested at multiple sampling times covering the time interval of 2 to

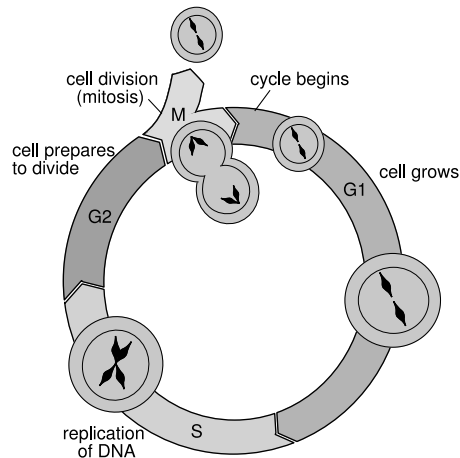


**Fig. 1** Schematic representation of the cell cycle consisting of 4 distinct phases, namely G1, S, G2 and M. For V79 cells used in the present study the mean duration times of the these phases are 2.25 h, 6.5 h, 1.5 h and 0.75h, respectively (Sinclair (1969); Scholz et al (1994)).

3 cell generation times. Each sampling time was preceded by a 2h colcemid treatment ( $0.1 \mu\text{mg ml}^{-1}$ ) to accumulate mitoses. Since the main purpose of the experiments was the analysis of the effect of cell cycle delays on the expression of cytogenetic damage, chromosome preparations were made according to the standard procedure and slides were stained with the fluorescence-plus-Giemsa technique. At each sampling time chromosomal damages was scored in 100 first cycle metaphases (Ritter et al (2000)). To gain information on the cell cycle progression, the mitotic index was determined for each sample by the direct scoring of 1000-2000 cells on the slides and the cell generation of at least 200 metaphases was recorded. Due to experimental limitation (access to the particle beam and number of cells that can be synchronized), more detailed measurements of the cell cycle progression, with a better time resolution, for example by flow cytometry, were not feasible. A detailed description of the experimental setup is given in (Ritter et al (2000)).

The passage through the cell cycle has been simulated by means of a kinetic model in which the duration of each phase is taken as a random variable characterized by its mean and dispersion (see below). The motivation for such an approach is the rapid radiation-induced desynchronization of initially synchronous cell populations. The cell-cycle time (the time interval between cell divisions) becomes then a random variable whose statistical properties can be inferred from the analysis of the frequencies of cells observed in different phases at different times. However, as mentioned above, the available information on the cell cycle kinetics relies solely on the measured mitotic indices. Therefore, for the analysis, these values were used to deduce (a posteriori) duration times in all phases before the mitosis. In the following sections, we aim to expand this approach and to present a model which is general enough to be applied not only for the analysis of radiation-induced cell cycle delays but also for the analysis of multi-compartment cell populations perturbed by other cancer therapies (Kohandel et al (2007)).

## 2.2 Mathematical model of cell cycle progression

In many experiments a positive correlation between radiation dose and the duration of cell-cycle delays was found. Although such findings were usually quantified in terms of a linear relationship between phase duration and dose (Zaider and Minerbo (1993); Hahnfeldt and Hlatky (1996)), a more detailed analysis points to a direct correlation between cell cycle delay and the number of aberrations carried by a cell (Gudowska-Nowak et al (2005)). This effect is responsible for the loss of synchrony of the population and can be illustrated by interpreting the (normalized) mitotic index as a frequency histogram of times spent by cells before the actual division happens. The cell cycle kinetics can be then investigated by treating the durations of the four phases as independent stochastic variables having probability density functions described in terms of two adjustable parameters (Zaider and Minerbo (1993); Montalenti et al (1998)). The parameters of such distributions are fixed in time (stationarity of the distribution is assumed), whereas the choice of a particular probability distribution function has been noted not to be critical for the final result (Hartmann et al (1975)).

For V79 Chinese hamster cells, as used in our simulations, the mean duration times of the cell cycle phases are  $t_{G1} = 2.25$  h,  $t_S = 6.5$  h,  $t_{G2} = 1.5$  h,  $t_M = 0.75$ h (Sinclair (1969); Scholz et al (1994)). The phase duration for an individual cell is given by a certain probability distribution  $D_{ph}(\tau)$ , where  $\tau$  is the time which a given cell had already spent in the current phase. Consequently, a single cell of phase age  $ph$  is assumed to leave its current phase within a time interval  $[\tau, \tau + d\tau]$  with a probability  $D_{ph}(\tau)d\tau$ . The mean number of cells  $dN_{ph \rightarrow}(t)$  leaving the phase  $ph$  within an infinitesimal time interval  $[t, t + dt]$  is defined by the mean flux  $\frac{dN_{ph \rightarrow}(t)}{dt}$ .

The experimental input to our model is given by the mitotic indices scored for exposed and control cell populations at subsequent 2h intervals (Ritter et al (2000)). Experimentally measured values of the mitotic index  $MI(i)$  at a timestep  $i$

$$MI(i) = \frac{N(i) - N(i-1)}{N(i-1)} \quad (1)$$

are defined as the increase in the total number of cells in relation to their number at the previous sampling time. Since the time until all cells reached the first mitosis was quite long compared to the average cycle length (Fig. 2), changes in the population size due to cell division have to be taken into account (Kaufman et al (1974); Scholz et al (1998)).

To determine the increase in the number of cells in relation to their initial number one expresses then the corrected mitotic index in the form

$$MI_{corrected}(i) = MI(i) \frac{N(i-1)}{N(0)} = \frac{N(i) - N(i-1)}{N(0)} \quad (2)$$

In turn, the summed mitotic indices up to the time step  $n$

$$S(n) = \sum_{i=0}^n MI_{corrected}(i) = \frac{N(n) - N_0}{N_0} \quad (3)$$

give then the fraction of cells which have already completed a full cycle, i.e. went through mitosis up to the given time. The experimental results show that this quantity

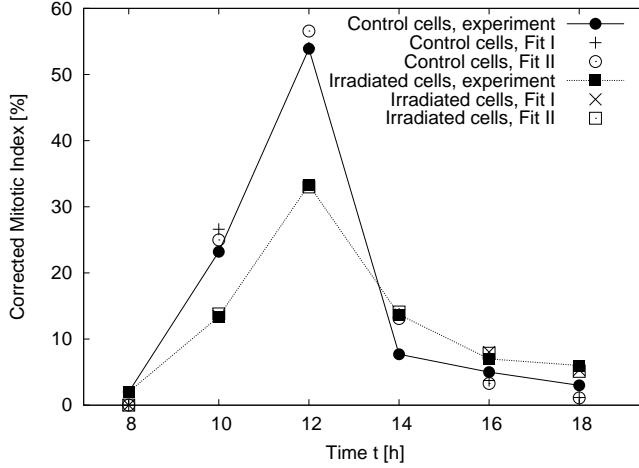


**Fig. 2** Corrected mitotic index of V79 cells exposed in  $G_1$  phase to 1.96 Gy Ar ions (10.4 MeV/u): experimental data (Gudowska-Nowak et al (2005); Ritter et al (2000)) along with fits and simulations of  $N_0 = 1000$  cells are shown. The mitotic index curve was fitted with a lognormal probability density function with parameters  $\mu$  and  $\sigma$  (cf. Eqs.(6, 7)) and the quality of the fit was determined by using the standard  $\chi^2$  test which yielded almost the same results in two cases. However, the underlying cell cycle kinetics is quite different for Fit 1 and Fit 2 (see Sec. 3 and Figs. 4, 5). In Fit 1, the  $G_1$  phase is largely dispersed whereas other phases have well defined duration times of negligible variance. In Fit 2 the phases S and G2 are dispersed and  $G_1$  and M duration times are assigned constant values.

tends to a constant level, which yields approximately 100% for control cells and less than 100% for irradiated cells, as displayed in Fig. 3.

The mean flux  $\frac{dN_{ph \rightarrow}(t)}{dt}$  defines a mean number of cells  $dN_{ph \rightarrow}(t)$  leaving the phase  $ph$  within an infinitesimal time interval  $[t, t + dt]$ . The term "mean" is understood here as an average over a large number of identical experiments, each with an initial number of  $N_0$  cells. Note that  $t$  stands here for the "absolute" time, different from the phase age  $\tau$ . In order to relate the description in terms of a mean flux  $\frac{dN_{ph \rightarrow}(t)}{dt}$  based on the ensemble approach to the description of the time evolution of a single cell whose probability of leaving the current phase is  $D_{ph}(\tau)$ , we assume that we deal with a large ensemble of samples, each initially containing  $N_0$  cells in the same phase  $ph$ . Moreover, the sample populations are assumed to be of the same phase age, e.g.  $\tau = 0$ . We start our "numerical experiment" at time  $t = 0$ , so that  $t = \tau$ , and count the cells which leave the phase within the age  $\tau$  and  $\tau + d\tau$ . Their mean number will be given by:

$$dN_{ph \rightarrow}^{(1)}(\tau) = N_0 F_{ph}(\tau) d\tau, \quad (4)$$

where  $F_{ph}(\tau)$  is a probability distribution which gives the likelihood of a cell leaving the phase at the time  $t = \tau$ .

On the other hand, if we trace the behavior of a particular cell, we can define  $D_{ph}(\tau)$  as the conditional probability distribution of leaving the phase at age  $\tau$ , provided that the cell had not completed the phase earlier:

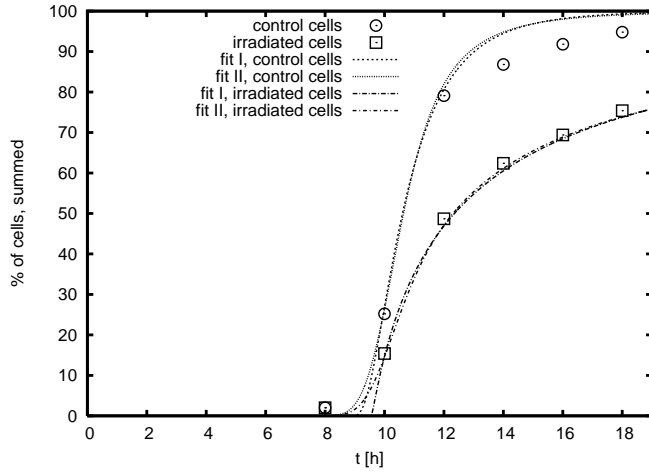


**Fig. 3** Cumulative fraction of cells which left the  $M$  phase of the first cycle, compared with the experimental results. For the explanation of fits, see Sec. 3

$$D_{ph}(\tau) = \frac{F_{ph}(\tau)}{1 - \int_0^\tau F_{ph}(\tau') d\tau'}. \quad (5)$$

Function  $F_{ph}(t)$  in the above formula represents the distribution of phase duration times in an initially synchronized population of cells. We follow the suggestions of Zaider and Minerbo (1993) and Montalenti et al. (1998) and assume a lognormal distribution of phase duration (Engen and Lande (1996)):

$$F_{ph}(t) = \frac{1}{t\sqrt{2\pi\sigma_{ph}^2}} \exp\left(-\frac{(\ln t - \mu_{ph})^2}{2\sigma_{ph}^2}\right). \quad (6)$$

with parameters  $\mu_{ph}$  and  $\sigma_{ph}$  determining the mean

$$E[t] = e^{\mu_{ph} + \frac{\sigma_{ph}^2}{2}} \quad (7)$$

and variance

$$E[(t - E[t])^2] = e^{2\mu_{ph} + \sigma_{ph}^2} (e^{\sigma_{ph}^2} - 1). \quad (8)$$

In the above expressions,  $\mu$  and  $\sigma$  are the parameters to be fitted.

It should be noticed that a log-normal distribution is not the only possible choice to be postulated as suitable for the description of the random distribution of phase duration times. The other possibility might be, e.g., the gamma distribution resulting from a mixture of exponential distributions expected in simple renewal processes (Feller (1968); Zaider and Minerbo (1993); Hahnfeldt and Hlatky (1996)).

Ensemble analysis of the mean flux allows splitting  $dN_{ph \rightarrow}(t)$  into a sum of contributions from subsequent cycles:

$$dN_{ph \rightarrow}(t) = \sum_{i=1} dN_{ph \rightarrow}^{(i)}(t) \quad (9)$$

$dN_{G1 \rightarrow}^{(1)}(t)$  is defined as the product of the probability of leaving the  $G1$  phase within the time interval  $(t, t + dt)$  and the mean total number of cells at time  $t$ :

$$dN_{G1 \rightarrow}^{(1)}(t) = dP_{G1 \rightarrow}(t)N(t), \quad (10)$$

which means that

$$dP_{G1 \rightarrow}(t) = F_{G1}(t)dt. \quad (11)$$

In the first cycle  $N(t) = N_0$ , so

$$dN_{G1 \rightarrow}^{(1)}(t) = dP_{G1 \rightarrow}^{(1)}(t)N_0 = N_0 dt F_{G1}(t). \quad (12)$$

The probability of leaving the  $S$  phase in the first cycle at a certain time will depend on the probability of leaving the previous phase, and thus

$$dN_{S \rightarrow}^{(1)}(t) = dP_{S \rightarrow}^{(1)}(t)N_0 = N_0 dt \int_0^t F_{G1}(t - \tau)F_S(\tau)d\tau = N_0 dt F_1(t), \quad (13)$$

and, analogously:

$$dN_{G2 \rightarrow}^{(1)}(t) = dP_{G2 \rightarrow}^{(1)}(t)N_0 = N_0 dt \int_0^t F_1(t - \tau)F_{G2}(\tau)d\tau = N_0 dt F_2(t), \quad (14)$$

$$dN_{M \rightarrow}^{(1)}(t) = dP_{M \rightarrow}^{(1)}(t)N_0 = N_0 dt \int_0^t F_2(t - \tau)F_M(\tau)d\tau = N_0 dt F_3(t). \quad (15)$$

In the moment of leaving the  $M$  phase, cells divide: two  $G1$  cells are produced and therefore, the number of cells in  $G1$  phase (and thus the number of those leaving  $G1$  phase) is twice larger:

$$dN_{G1 \rightarrow}^{(2)}(t) = 2dP_{G1 \rightarrow}^{(2)}(t)N_0 = 2N_0 dt \int_0^t F_3(t - \tau)F_{G1}(\tau)d\tau = 2N_0 dt F_4(t). \quad (16)$$

In this manner we generate consecutive contributions to Eq. (9). Knowing the mean flux as given by Eq. (9) we can calculate other mean quantities of interest, such as mean number of cells found in the phase  $ph$  at a given time after irradiation. This method gives therefore a global view on the cell cycle kinetics.

In order to reconstruct the fate of an individual cell, we have used the Monte Carlo method. The computer simulation tracks the cycle of each single cell separately. Initially we generate an ensemble of  $N_0$  cells. Each cell is assumed to start in the  $G1$  phase and its phase age is  $\tau = 0$ . In subsequent time steps each cell goes through its individual cycle, and in every time step  $d\tau$  each cell has a probability  $D_{ph}(\tau)d\tau$  to leave its current phase. The algorithm is built based on the following scheme:

1. The cell is in the phase  $ph$ . Its phase age is  $\tau$ .
2. A random number  $x$ ,  $0 \leq x < 1$  is generated.
3. If  $x < D_{ph}(\tau)d\tau$ , the programme proceeds to 4., else it goes to 6.
4. If the next phase " $ph + 1$ "  $\neq G1$ , then the cell exits from its current phase:  $ph = "ph + 1"$ ,  $\tau = 0$ . Go to 1.
5. If the next phase " $ph + 1$ " =  $G1$ , then the cell exits from its current phase and replicates:  $ph = G1$ ,  $\tau = 0$ . Additionally, a new cell is generated, whose current phase is  $G1$  and  $\tau = 0$ . The cycle starts with going to 1.
6. The cell remains in its current phase:  $\tau = \tau + d\tau$ . At the next step the programme



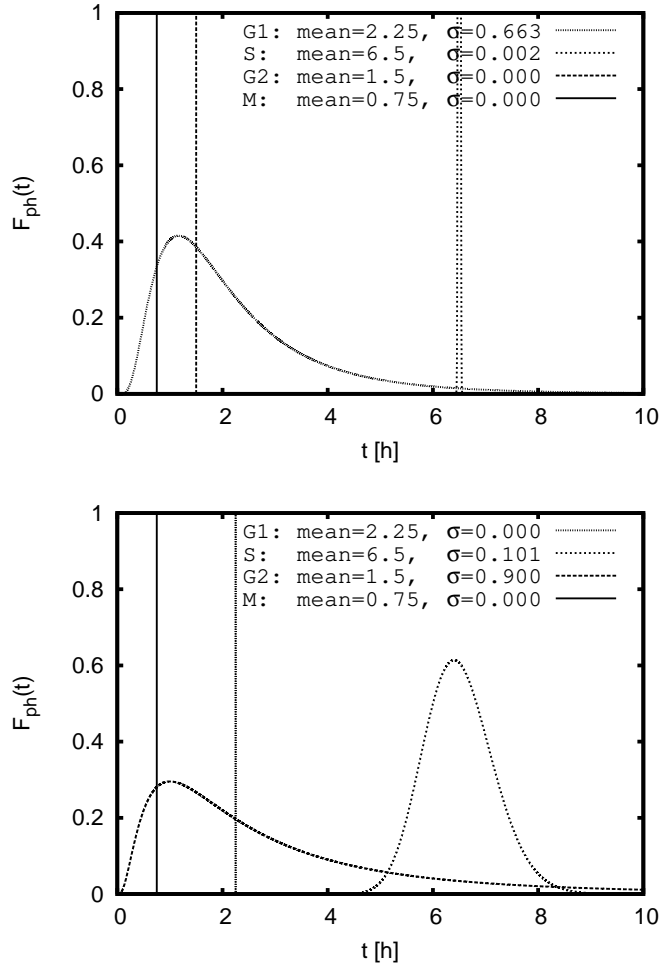


**Fig. 4** Control cells: Probability density functions for leaving a phase in phase age  $\tau$  (top panel: Fit 1, bottom panel: Fit 2)

starts with 1.

All integrations to compute  $D_{ph}(\tau)$  from (5) have been performed in our simulation using the Euler method with discrete time steps  $\Delta t$ .

The above described approach allows to examine the kinetics of a single experiment. Computing the variance of quantities of interest, we can estimate how much a single realization of the experiment deviates from the ensemble average.

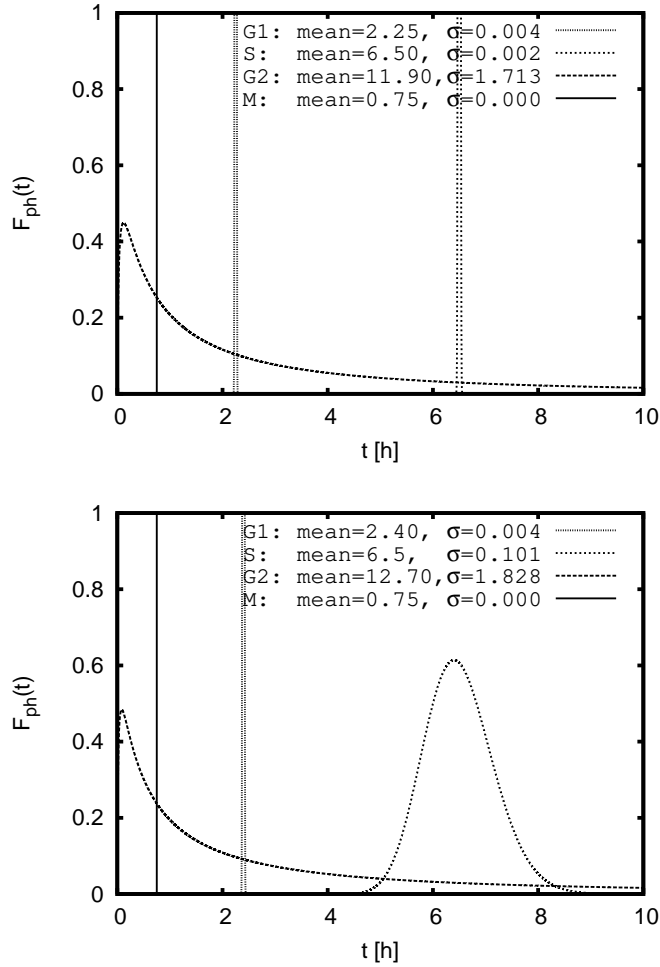


**Fig. 5** Irradiated cells: Probability density functions for leaving a phase in phase age  $\tau$  (top panel: Fit 1, bottom panel: Fit 2), cf. Eqs. (18, 19).

### 3 Results

Using the methods described above, we have first fitted the experimental results, i.e. the mitotic indices (see Sec. 2.1). Since the experimentally accessible information refers to cells initially synchronized in G1 phase, we assumed an "ideal synchrony" for the numerical analysis, i.e. at time  $t = 0$  all of cells were assumed to be of the phase age  $\tau = 0$ .

Control cells						
Phase	Fit I			Fit II		
	Median	Mode	CV	Median	Mode	CV
G1	1.806	1.164	1.346	2.25	2.25	-
S	6.500	6.500	500	6.467	6.401	9.876
G2	1.5	1.5	-	1.000	0.445	0.895
M	0.75	0.75	-	0.75	0.75	-
Irradiated cells						
Phase	Fit I			Fit II		
	Median	Mode	CV	Median	Mode	CV
G1	2.250	2.250	250	2.398	2.398	250
S	6.500	6.500	500	6.467	6.401	9.876
G2	2.744	0.146	0.237	2.389	0.084	0.192
M	0.75	0.75	-	0.75	0.75	-

**Table 1** Median, modal values and coefficients of variation for the fitted phase duration time distributions  $F_{ph}$ .

### 3.1 Control cells

The first step in our analysis was fitting the parameters of the  $F_{ph}$  distributions (6) for each phase, in such a way that they together made up the time-course of mitosis (15) which fitted the experimental corrected mitotic indices (2).

We performed the integrations numerically with a time-step  $\Delta t = 0.03$  h (Euler method), obtaining an approximate flux:

$$\frac{\Delta N_{ph \rightarrow}(t)}{\Delta t} \approx \frac{dN_{ph \rightarrow}(t)}{dt}. \quad (17)$$

Having evaluated the outflow from the M phase, we could further easily compute the total mean number of cells at a given time, from which the (mean) corrected mitotic index (2) was constructed. (We recall that the word "mean" is understood here as an average over a large number of identical experiments.)

Since we would have had to fit up to 8 parameters, we decided to simplify the task. The results cited in Sec. 2.1 delivered the values of mean duration times of each phase:  $\bar{t}_{G1} = 2.25$  h,  $\bar{t}_S = 6.5$  h,  $\bar{t}_{G2} = 1.5$  h,  $\bar{t}_M = 0.75$ h. Therefore, we used them as the four (frozen) parameters needed for modelling and focused on four others (we chose  $\sigma_{ph}$ , which can be treated as a measure of fitted distribution's width) which had to be chosen by the best fit. The initial number of cells assumed for the modelling was  $N_0 = 1000$  and the parameters were fitted by using a Metropolis algorithm.

We found that the result of the fitting (see Fig. 2) was ambiguous and there were two possible least-square fits with  $\chi^2$  value of the same order. The inferred coefficients displayed a significant variability between both data sets (see Fig. 4 and Tab. 1):

Fit 1:

$$\sigma_{G1} = 0.663, \sigma_S = 0.002, \sigma_{G2} = 0.000, \sigma_M = 0.000, \chi^2 = 55.0 \quad (18)$$

Fit 2:

$$\sigma_{G1} = 0.000, \sigma_S = 0.101, \sigma_{G2} = 0.900, \sigma_M = 0.000, \chi^2 = 50.0 \quad (19)$$

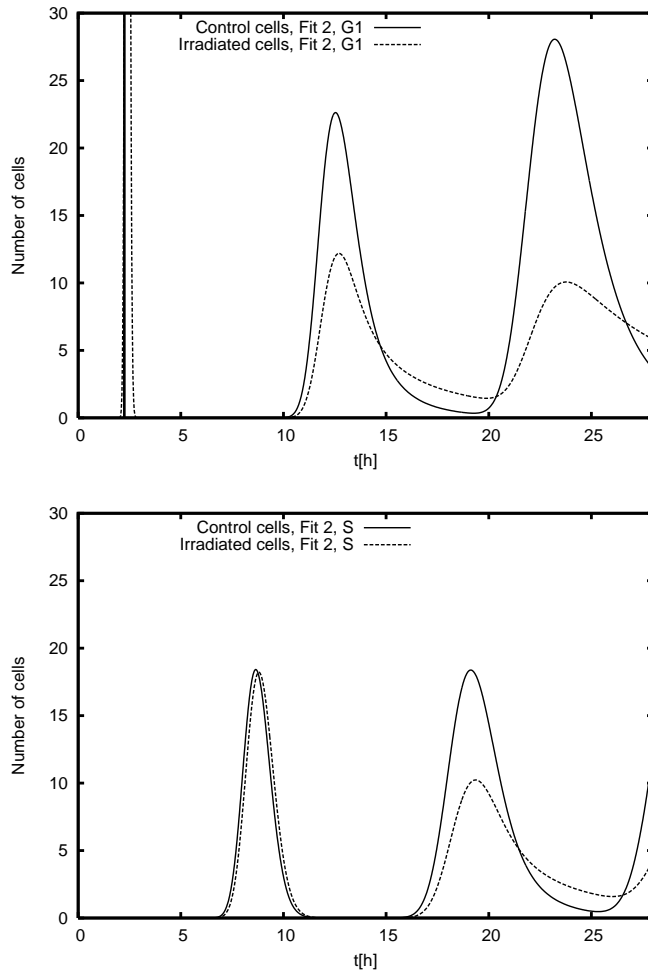


**Fig. 6** Flux from phases G1 and S (number of cells passing per 1h) at time  $t$ , compared for control and irradiated cells (Fit 2).

Although the two possible cell cycle schemes produced almost identical mitotic index curves, the intra-cycle distributions differed very much. In Fit 1, the G1 phase is largely dispersed whereas other phases have well-defined (deterministic) duration times. In contrast, in Fit 2, S and G2 phases are dispersed with the duration times of G1 and M phases being well specified.

### 3.2 Irradiated cells

In order to reproduce the mean corrected mitotic indices of the irradiated cell population we performed a similar fitting procedure as mentioned above. To proceed, we made the biologically justified assumption that irradiation affects only the characteristics of

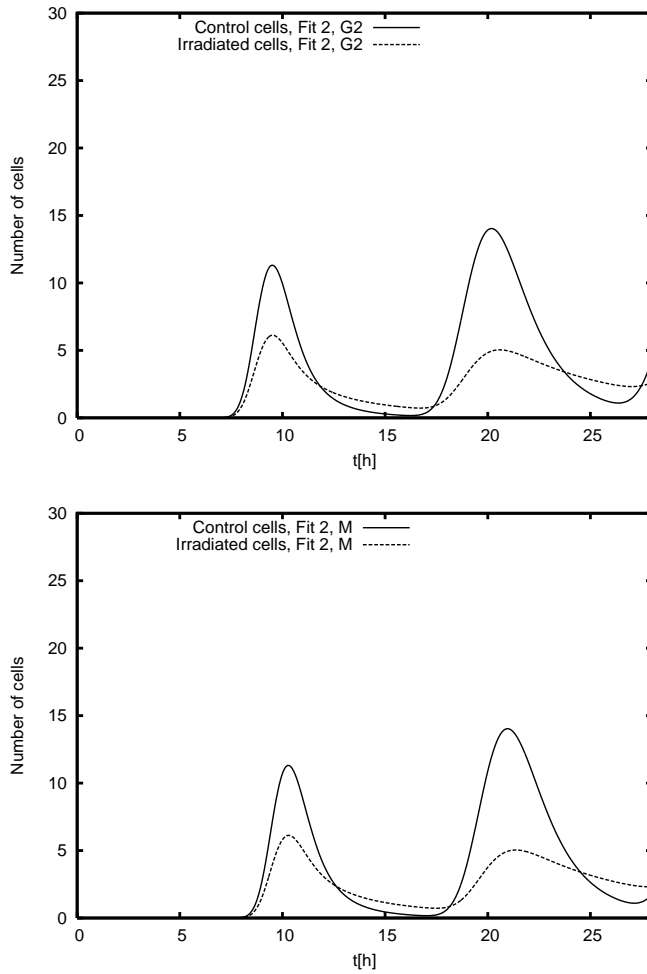


**Fig. 7** Flux from phases G2 and M (number of cells passing per 1h) at time  $t$ , compared for control and irradiated cells (Fit 2).

G1 and G2 phases, since checkpoints in G1 and G2 are known to block the cell cycle progression to give the cell time to repair and continue cycling or to undergo apoptosis (Li and Zou (2005)). We also expected that the mean duration times of both phases, as well as the variances of the duration times should increase because the damaged cells would be blocked in either one of them for a longer time. Therefore, we fitted only the parameters  $\bar{t}_{G1}, \sigma_{G1}, \bar{t}_{G2}, \sigma_{G2}$ , taking others as fixed and referring to their values obtained in the former fit for control cells. While doing so, we did not introduce any additional mortality parameter. Instead, we assumed solely that the damaged cells will stay in G1 or G2 phase for a very long time.

For the parameters corresponding to Fit 1 the analysis yielded:

$$\bar{t}_{G1} = 2.25, \sigma_{G1} = 0.004, \bar{t}_{G2} = 11.90, \sigma_{G2} = 1.713, \chi^2 = 5.6, \quad (20)$$

whereas for Fit 2 it resulted in:

$$\bar{t}_{G1} = 2.40, \sigma_{G1} = 0.004, \bar{t}_{G2} = 12.70, \sigma_{G2} = 1.828, \chi^2 = 5.8 \quad (21)$$

In both fits the  $F_{G2}(\tau)$  distribution function became wider and its mean duration time strongly increased (Fig. 5, see also Tab. 1).

In turn, the  $F_{G1}(\tau)$  distribution in Fit 1 became narrower in comparison to the corresponding distribution for the control cells, which implied that Fit 1 was unrealistic. This finding is consistent with previous flow cytometric studies showing that V79 cells suffer short cell cycle delays in G1 phase, but more pronounced delays in S- or G2-phase (Scholz et al. 1994). The low activity of the G1 checkpoint in V79 cells might result from mutations in the p53 gene (Chaung et al, 1997). We have therefore concluded that Fit 2 was confirmed as better matching the biological scenario: here the mean duration time of G1 increased and the distribution function became wider. The very long tail of  $F_{G2}(\tau)$ , as predicted in this case, suggests that damaged cells may remain blocked in the G2 phase for an extremely long time with a non-zero probability as it has been experimentally shown by Scholz et al. (1994).

Figs. 6 and 7 compare the progression of cell fluxes between subsequent phases for control and irradiated populations, respectively, while the number of cells remaining in a given phase at time  $t$  is shown in Figs. 8 and 9. In the first cell cycle a notably slower outflow of cells from the G2 phase is visible which corroborates with the number of cells remaining in that phase up to 16h after exposure. Cells blocked in that phase also diminish the fraction of those which are able to enter mitosis up to the same time-point. As expected, the cumulative number of cells which enter mitosis is much lower in the irradiated population than in the control sample and can be well correlated with the fraction of cells arrested in G2.

### 3.3 Determination of experimental errors

Another important finding of our work is that the applied approach allows for estimation of inter-experimental differences resulting from the stochastic character of phase duration times. By performing a Monte Carlo simulation, described in Sec. 2.2 we simulated a time-evolution of an ensemble of cells (here:  $N_0 = 1000$ ) using the set of previously fitted parameters. The number of cells at different moments of time was counted, and therefrom the mitotic index (1) was derived. Using this method, the variance/standard deviation of the corresponding probability distribution function was estimated (see Fig. 11).

We performed a series of 100 cell cycle simulations with the initial number of cells  $N_0$ . The mean number of cells found in a given phase  $\langle N_{ph}(t) \rangle$  and the variance  $\sigma_{N_{ph}}^2(t)$  were calculated. Analyzing the mutual dependence of the relative error  $\frac{\sigma_{N_{ph}}}{\langle N_{ph} \rangle}$  and  $\langle N_{ph} \rangle$  we found that the relative error does not depend on the initial number of cells  $N_0$  nor on the set of parameters of  $F_{ph}$ . It depends only on the current number of cells. A practical conclusion drawn from these results is that the number of cells analyzed in an experimental sample should be at least of order of 100 to obtain a

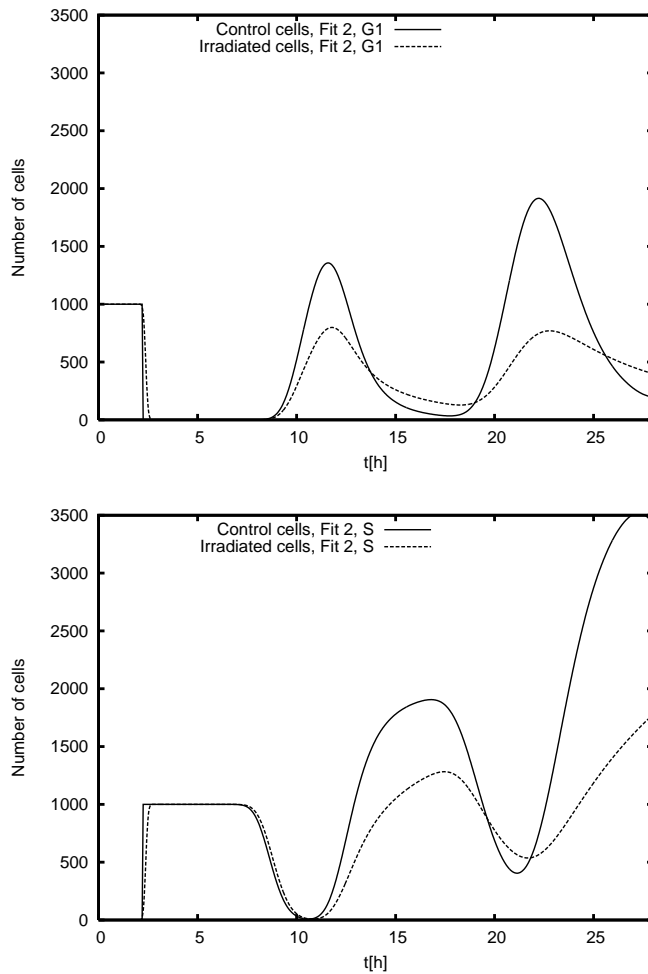


**Fig. 8** Number of cells in phases G1 and S at time  $t$ , compared between control and irradiated cells (Fit 2).

relative error less than 20%. If a better precision is required, a larger cell population has to be examined.

#### 4 Discussion

In studies preceding this project (Ritter et al (1996, 2000); Scholz et al (1998); Gudowska-Nowak et al (2005)) the relationship between radiation-induced mitotic delay and expression of chromosome damage was shown. To further establish differences in progression through the division cycle of unirradiated (control) and exposed cells, we developed a method for retrieval of the information about the time-course of all cell cycle phases, when only the mitotic index of a cell sample is known. The method consists in a multi-

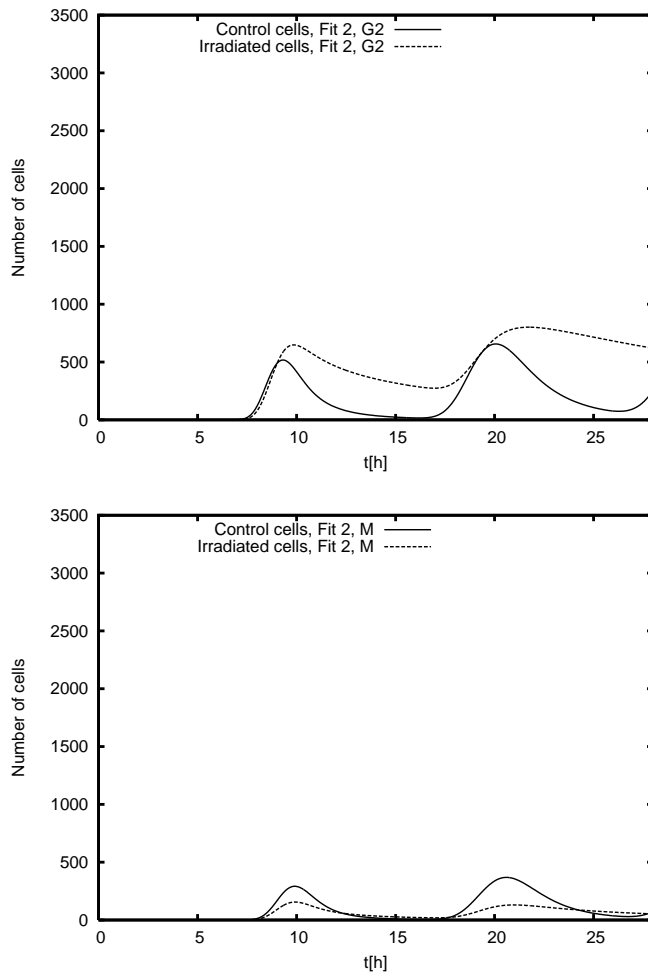


**Fig. 9** Number of cells in phases G2 and M at time  $t$ , compared between control and irradiated cells (Fit 2).

dimensional fit based on general assumptions concerning the duration distribution of cell cycle phases, which are inferred from other experiments (Montalenti et al, 1998).

The analysis of the experimentally measured mitotic indices for mammalian V79 cells after exposure to Ar ions (Ritter et al (2000)) revealed a prolonged block of damaged cells in the G2 phase. Additionally, we have shown that this approach is applicable directly to determine experimental errors resulting from the stochastics of phase duration times.

In future studies the quality of the model will be validated through the application to data sets generated for other cell lines and cell types such as human skin fibroblasts and lymphocytes whose cell-cycle kinetics after irradiation is altered differently (Flatt et al (1998); Lee et al (2005); Tenhumberg et al (2007)). For example, it has been shown that normal human fibroblasts exposed in G0/G1 phase to ionizing radia-



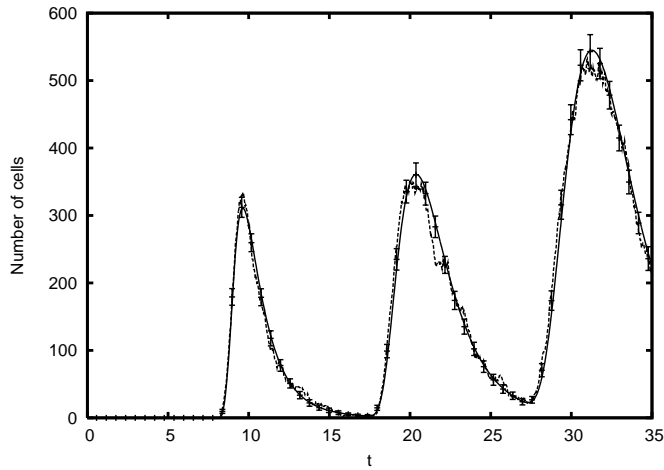


**Fig. 10** Number of cells found in M phase at time  $t$ . Black line: theoretical prediction obtained using the mean flux approach. Dashed line: a single simulation for  $N_0 = 1000$  cells. Error bars: standard deviation for the simulation.

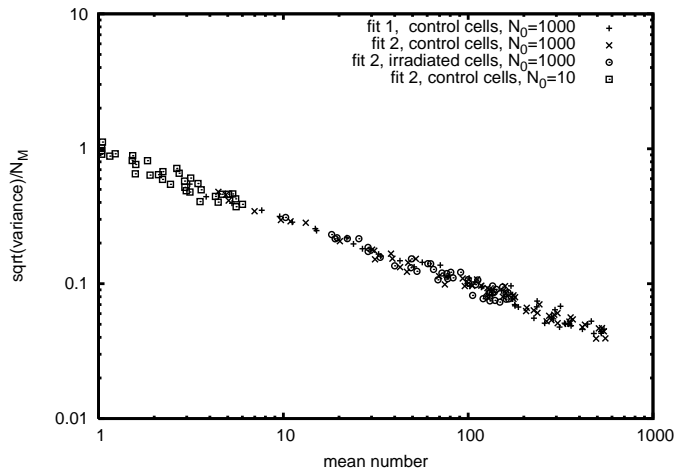


**Fig. 11** Relative error of the measurement vs. mean total number of cells analyzed.

tion suffer a prolonged G1 arrest (Flatt et al (1998); Tenhumberg et al (2007)), while human lymphocytes are predominantly arrested in G2 (Lee et al (2005)). Furthermore, the model may be used to analyze the progression of cells carrying different numbers of aberrations.

---

## References

- Amaldi U, Kraft G (2007) European developments in radiotherapy with beams of large radiobiological effectiveness. *J Radiat Res (Tokyo)*, Suppl A 48:27–41
- Basse B, Ubezio P (2007) A generalised age- and phase-structured model of human tumour cell populations both unperturbed and exposed to a range of cancer therapies. *Bull Math Biol* 69:1673–1690
- Cucinotta FA, Durante M (2006) Cancer risk from exposure to galactic cosmic rays: implications for space exploration by human beings. *Lancet Oncol* 7:431–435
- Engen S, Lande R (1996) Population dynamic models generating the lognormal species abundance distribution. *Math Biosci* 132:169–183
- Erba E, Bassano L, Liberti GD, Muradore I, Chiorino G, Ubezio P, Vignati S, Codegoni A, Desiderio MA, Faircloth G (2002) Cell cycle phase perturbations and apoptosis in tumour cells induced by apolidine. *British Journal of Cancer* 86:1510–1517
- Feller W (1968) An introduction to probability theory and its applications. John Wiley, New York
- Flatt P, Price J, Shaw A, Pietenpol J (1998) Differential cell cycle checkpoint response in normal human keratinocytes and fibroblasts. *Cell Growth Differ* 9:535–543
- Groesser T, Chun E, Rydberg B (2007) Relative biological effectiveness of high-energy iron ions for micronucleus formation at low doses. *Radiat Res* 168:675–682
- Gudowska-Nowak E, Kleczkowski A, Nasonova E, Scholz M, Ritter S (2005) Correlation between mitotic delay and aberration burden, and their role for the analysis of chromosome damage. *Int J Radiat Biol* 81:23–32
- Hahnfeldt P, Hlatky L (1996) Resensitization due to redistribution of cells in phases of the cell cycle during arbitrary radiation protocols. *Radiat Res* 145:134–143
- Hartmann N, Gilbert C, Jansson B, Macdonald PDM, Steel G, Valleron A (1975) A comparison of computer methods for the analysis of fraction labelled mitoses curves. *Cell Tissue Kinet* 8:119–124
- Kaufman G, Miller M, Savage J, Papworth D (1974) Chromosome aberration yields from multiple fixation regimes. *J Theoret Biol* 44:91–103
- Kohandel M, Kardar M, Milosevic M, Sivaloganathan S (2007) Dynamics of tumor growth and combination of anti-angiogenic and cytotoxic therapies. *Phys Med Biol* 52:3665–3677
- Lee R, Nasonova E, Ritter S (2005) Chromosome aberration yields and apoptosis in human lymphocytes irradiated with Fe-ions of differing LET. *Adv Space Res* 35:268–275
- Li L, Zou L (2005) Sensing, signaling, and responding to DNA damage: organization of the checkpoint pathways in mammalian cells. *J Cell Biochem* 94:298–306
- Mateuca R, Lombaert N, Aka PV, Decordier I, Kirsch-Volders M (2006) Chromosomal changes: induction, detection methods and applicability in human biomonitoring. *Biochimie* 88:1515–1531
- Montalenti F, Sena G, Capella P, Ubezio P (1998) Simulating cancer cell kinetics after drug treatment: application to cisplatin on ovarian carcinoma. *Phys Rev E* 57:5877–5887
- Pathak R, Dey S, Sarma A, Khuda-Bukhsh A (2007) Genotoxic effects in M5 cells and Chinese hamster V79 cells after exposure to  $^7\text{Li}$ -beam (LET=60 keV/micron) and correlation of their survival dynamics to nuclear damages and cell death. *Mutat Res* 628:56–66

- 
- Purrot R, Vulpis N, Lloyd D (1980) The use of harlequin staining to measure delay in the human lymphocyte cell cycle induced by in vitro X-irradiation. *Mutat Res* 69:275–282
- Ritter S, Nasonova E, Scholz M, Kraft-Weyrather W, Kraft G (1996) Comparison of chromosomal damage induced by X-rays and Ar ions with an LET of 1840 keV/ $\mu\text{m}$  in G1 V79 cells. *Int J Radiat Biol* 69:155–166
- Ritter S, Nasonova E, Gudowska-Nowak E (2000) Effect of LET on the yield and the quality chromosomal damage in metaphase cells: a time-course study. *Int J Radiat Biol* 78:191–202
- Scholz M (2003) Effects of ion radiation on cells and tissues. *Advances in Polymer Science* 162:95–155
- Scholz M, Kraft-Weyrather W, Ritter S, Kraft G (1994) Cell cycle delays induced by heavy ion irradiation of synchronous mammalian cells. *Int J Radiat Biol* 66:59–75
- Scholz M, Ritter S, Kraft G (1998) Analysis of chromosome damage based on the time course of aberrations. *Int J Radiat Biol* 74:325–331
- Sinclair WK (1969) Protection by cysteamine against lethal X-ray damage during the cell cycle of Chinese hamster cells. *Radiat Res* 39:135–154
- Tenhumberg S, Gudowska-Nowak E, Nasonova E, Ritter S (2007) Cell cycle arrest and aberration yield in normal human fibroblasts. II: Effects of 11 MeV  $\text{u}^{-1}$  C ions and 9.9 MeV  $\text{u}^{-1}$  Ni ions. *Int J Radiat Biol* 83:501–513
- Virgilio AD, Iwami K, Wätjen W, Kahl R, Degen G (2004) Genotoxicity of the isoflavones genistein, daidzein and equol in V79 cells. *Toxicol Lett* 151:151–162
- Weyrather W, Ritter S, Scholz M, Kraft G (1999) RBE for carbon track-segment irradiation in cell lines of differing repair capacity. *Int J Radiat Biol* 75:1357–1364
- Wilson G (2007) Cell kinetics. *Clin Oncol* 19:370–384
- Zaider M, Minerbo GN (1993) A mathematical model for cell cycle progression under continuous low-dose-rate irradiation. *Radiat Res* 133:20–26